The Whole Is Not the Simple Sum of Its Parts in Calmodulin from *S. cerevisiae*†

Sandra Y. Lee and Rachel E. Klevit*

Department of Biochemistry, Biomolecular Structure Center, Box 357742, University of Washington, Seattle, Washington 98195-7742

Received November 23, 1999

ABSTRACT: Calmodulin is an essential Ca^{2+}-binding protein involved in a multitude of cellular processes. The calmodulin sequence is highly conserved among all eukaryotic species; calmodulin from the yeast *S. cerevisiae* (yCaM) is the most divergent form, while still sharing 60% sequence identity with vertebrate calmodulin (vCaM). Although yCaM can be functionally substituted by vCaM in vivo, the two calmodulin proteins possess significantly different Ca^{2+}-binding properties as well as abilities to activate vertebrate target enzymes in vitro. In addition, it has been observed that certain properties of the N-terminal and C-terminal domains of Ca^{2+}-yCaM differ depending on whether they are in the context of the whole protein or isolated as half-molecule fragments. To investigate the structural basis for these differing properties, we have undertaken nuclear magnetic resonance (NMR) studies on yCaM and the two half-molecule fragments representing its two individual domains, yTr1(residues 1−76) and yTr2 (residues 75−146). We present direct evidence that the two domains of Ca^{2+}-yCaM interact via their exposed hydrophobic surfaces. Thus, the Ca^{2+}-bound form of yCaM exists in a novel compact structure in direct contrast to the well-established structure of Ca^{2+}-vCaM comprised of two independent globular domains.

Calmodulin's role as a Ca^{2+}-signal transduction protein depends on its ability to couple the transient fluxes of intracellular Ca^{2+} levels to the regulation of various target proteins and thus cellular processes (*1*−*4*). The protein accomplishes this by linking its Ca^{2+}-binding process to the conformational change it undergoes that exposes a hydrophobic surface with which it interacts and regulates a number of its target proteins (*5*). The structure of calmodulin must, therefore, be optimized to act as a Ca^{2+}-signal transduction protein in a number of pathways, suggesting that the amino acid sequence of this protein has evolved to an optimal state. Indeed, the sequence of calmodulin is distinguished by a high degree of conservation among all eukaryotic species. The sequences from all vertebrate species are identical, while they are still greater than 90% identical when all multicellular eukaryotes from insects to plants are considered (*6*). The most divergent form of calmodulin is from the budding yeast *S. cerevisiae* with 60% sequence identity and even higher sequence homology (*6*, *7*).

As a reflection of its sequence divergence, yCaM[1] displays certain biochemical properties that are distinctly different from vCaM. Most notable is the fact that yCaM binds only three Ca^{2+} ions instead of the four seen in all other calmodulins (*8*, *9*). Results from mutagenesis, limited proteolysis, and NMR studies established that EF-hand site IV is unable to bind Ca^{2+} (*9*−*11*), presumably a consequence of two amino acid sequence differences: (1) the invariant Ca^{2+}-binding Glu at the 12th position is a Gln and (2) a one amino acid deletion within the Ca^{2+}-binding loop. A second notable difference between yCaM and vCaM is that the former displays cooperativity of Ca^{2+} binding among all three sites, whereas vCaM displays cooperativity only between the two EF-hand motifs that make up the N-terminal or C-terminal domains (*9*, *12*).

yCaM is also distinguished from vCaM in its functional abilities as it is less effective at activating the target proteins of vCaM in vitro despite the fact that vCaM can replace yCaM in vivo (*8*, *13*, *14*). For example, Ca^{2+}-yCaM activates myosin light chain kinase only to ∼13% of maximum activity, and a 1000-fold molar excess of Ca^{2+}-yCaM is required for maximal activation of phosphodiesterase. Mutagenesis and protein hybrid experiments suggest that the inability of the EF-hand site IV to bind Ca^{2+} is responsible for Ca^{2+}-yCaM's inability to activate Ca^{2+}-vCaM's target enzymes (*15*).

Functional differences between yCaM and vCaM are likely to arise from structural differences in the Ca^{2+}-bound form of the two proteins. Ca^{2+}-induced changes in the circular dichroism (CD) spectra of yCaM provided the first indication of such a difference (*10*, *13*). The addition of Ca^{2+} to vCaM causes an increase in ellipticity, while Ca^{2+} binding to yCaM causes a decrease. Although increases in the ellipticity at 222 nm are usually associated with increased α-helical content, it can also indicate a reorientation of helical secondary structural elements. This is especially true in the case of calmodulin, since a comparison of the structures of apo-vCaM and Ca^{2+}-vCaM do not reveal any net increase in helical content but instead show a reorientation of the helices from an antiparallel arrangement in the apo form to a perpendicular arrangement in the Ca^{2+}-bound form (*16*, *17*). X-ray scattering measurements indicate that Ca^{2+}-yCaM exists in a more compact conformation than the Ca^{2+}-free form, in contrast to what is known about the structure of

† This work was supported by NIH Grant R01 DK35187 to R. E. K.

* To whom correspondence should be addressed. E-mail: klevit@u.washington.edu.

[1] Abbreviations: yCaM, *S. cerevisiae* calmodulin; vCaM, vertebrate calmodulin; NMR, nuclear magnetic resonance; yTr1, N-terminal domain fragment of yCaM (1−76); yTr2, C-terminal domain fragment of yCaM (75−146); CD, circular dichroism; 1D, one-dimensional; vTr1, N-terminal domain fragment of vCaM; vTr2, C-terminal domain fragment of vCaM; HSQC, heteronuclear single quantum correlation; K_d, disassociation constant.

10.1021/bi992697a CCC: $19.00
Published on Web 03/22/2000

Ca^{2+}-vCaM (*18*). Both X-ray scattering and NMR relaxation measurements of Ca^{2+}-vCaM indicate an extended bilobular protein conformation in which the two domains tumble independently of one another (*19*, *20*). Ca^{2+}-vCaM's conformation becomes more compact only when it is bound to a peptide representing its binding site on a target enzyme (*20*).

A number of observations have revealed that certain properties of the N-terminal and C-terminal domains of Ca^{2+}-yCaM differ depending whether they are in the context of the whole protein or isolated as half-molecule fragments. For example, the dissociation constants for Ca^{2+} binding to yCaM range from 2.0 to 5.0 μM, versus 1.2 and 13.0 μM for the N-terminal fragment and 5.2 μM for the C-terminal fragment (*9*, *21*). In contrast, it is well established that the Ca^{2+}-binding affinities for each pair of EF-hand motifs in vCaM are the same whether in the context of the whole protein or isolated as a half-molecule fragment (*12*). Context-dependent Ca^{2+}-binding properties of yCaM and context-independent Ca^{2+}-binding properties of vCaM are also apparent from spectral perturbations observed in 1D ^{1}H NMR Ca^{2+} titrations of yCaM, vCaM, and their respective half-molecule fragments. For example, the His 107 peak from whole yCaM displays slow-exchange behavior, whereas in yTr2 the His 107 peak titrates in the fast-exchange regime (*9*, *21*). For vCaM, it has been shown that the fast-exchange behavior of the N-terminal domain peaks and the slow-exchange behavior of the C-terminal domain peaks exist in both the whole vCaM protein and the half-molecule fragments (*22*).

Given the overwhelming evidence for biochemical, functional, and structural differences between Ca^{2+}-yCaM and Ca^{2+}-vCaM, we undertook NMR studies on Ca^{2+}-yCaM to investigate the structural basis for the differing properties. ^{1}H-^{15}N HSQC spectra of Ca^{2+}-yCaM indicated the presence of chemical exchange broadening, making a conventional NMR analysis of Ca^{2+}-yCaM challenging. Therefore, we used half-molecule fragments representing the two individual domains of yCaM, yTr1 (residues 1−76) and yTr2 (residues 75−146) to probe the structural differences between the isolated domain fragments and the whole Ca^{2+}-yCaM. Our NMR data indicate that the structures of the two domains in the Ca^{2+}-bound form are indeed different depending on whether they are isolated half-yCaM fragments or in the context of the whole yCaM protein. We present the first direct evidence that this structural difference is due to an interaction between the two domains of Ca^{2+}-yCaM and suggest a functional significance for the interaction.

MATERIALS AND METHODS

Sample Preparation. Expression and purification protocols for yCaM, yTr1, and yTr2 have been described (*9*). When purifying yTr1 and yTr2, the wash buffer for the second Phenyl-Sepharose column consisted of 50mM Tris, pH 7.5, 10mM Ca^{2+}, and 800mM $(NH_4)_2SO_4$, and the elution buffer consisted of 50mM Tris, pH 7.5, 50mM EGTA, and 800mM $(NH_4)_2SO_4$. A G75 Sephadex sizing column step was added to remove high molecular weight contaminants. The purified protein was passed over a Chelex column to remove trace amounts of Ca^{2+}. Uniformly ^{15}N-labeled proteins were prepared by growing the cells in M9 medium supplemented with $^{15}NH_4Cl$. The constructs for vCaM, vTr1, and vTr2 were a generous gift from M. Shea (*23*). Expression and purification of these proteins followed previously described protocols except that (1) the wash and elution buffers for the second Phenyl-Sepharose column were those used in the yTr1 and yTr2 protocol, and (2) a G75 Sephadex sizing column and a Chelex column were used as above. Uniformly ^{15}N-labeled vTr1 and vTr2 were prepared by growing the cells in MOPS buffer supplemented with $^{15}NH_4Cl$ (*24*). NMR samples contained either 0.5 mM or 1.0 mM protein dissolved in 90%H_2O/10%D_2O containing 50 mM imidazole, 100 mM KCl, pH 6.1. Ca^{2+} was added to the NMR samples to a final concentration of 5mM.

NMR Spectroscopy. NMR spectra were acquired at 22 °C on a Bruker DMX-500 instrument, unless otherwise noted. ^{1}H-^{15}N HSQC spectra were collected with 256 t_1's and 16 scans per t_1. For line-width measurements, an HSQC with 600 t_1 increments was collected. Spectral widths of 6410 Hz for the ^{1}H dimension, 1216 Hz for the ^{15}N dimension in the Ca^{2+}-free spectra, and 1470 Hz for the ^{15}N dimension in the Ca^{2+}-bound spectra were used. Our ^{1}H-^{15}N HSQC spectrum contained the expected number of cross-peaks, whereas the published backbone assignments of Ca^{2+}-yTr1 are incomplete, necessitating reassignment of our ^{1}H-^{15}N HSQC spectrum (*25*). Complete backbone NH assignments were made (with the exception of the first three residues) based on a 2D ^{1}H-^{15}N HSQC-TOCSY and a ^{1}H-^{15}N 3D NOESY−HSQC (collected at 750 MHz on a Bruker DMX750).

^{1}H-^{15}N HSQC Titration Experiments. Titration experiments were performed on 0.5 mM NMR samples of ^{15}N-labeled Ca^{2+}-yTr1 or Ca^{2+}-yTr2 by recording a series of 2D ^{1}H-^{15}N HSQC spectra in the presence of increasing amounts of unlabeled Ca^{2+}-yTr2 for the ^{15}N-yTr1 titration experiment, unlabeled Ca^{2+}-yTr1 for the ^{15}N-yTr2 titration experiment, and unlabeled Ca^{2+}-vTr2 for the ^{15}N-yTr1 control experiment. Up to 18 mole equiv of unlabeled yTr2 were added during the ^{15}N-yTr1 titration; 14 mole equiv of unlabeled yTr1 were added during the ^{15}N-yTr2 titration; and 17 mole equiv of unlabeled vTr2 was added in the ^{15}N-yTr1 control experiment. The protein samples and the stock solution of the unlabeled domains were prepared in the same NMR buffer to maintain buffer conditions throughout the titration.

Fitting of Chemical Shift Perturbations to Binding Curve. The chemical shift changes of fast exchanging yTr1 peaks were fit using the program Xcrvfit (*26*) (PENCE/MRC group Joint Software Centre). The total chemical shift difference was set as the chemical shift difference between the Ca^{2+}-yTr1 peaks in the presence of 0 equiv of unlabeled yTr2, the beginning point of the titration experiment and the corresponding Ca^{2+}-yCaM peak, the putative end point of the titration experiment. This value was held constant during the fitting. Only data from peaks whose corresponding Ca^{2+}-yCaM peaks were unambiguous were used in the analysis.

RESULTS AND DISCUSSION

As a first step toward determining the structure of yeast calmodulin, we collected NMR spectra of ^{15}N-labeled yCaM, yTr1, and yTr2. The ^{15}N-labeled fragments provide an opportunity to detect structural differences between the isolated domain fragments and the whole calmodulin protein. For example, consistent with the published structures of vCaM revealing two noninteracting globular domains linked by a central, flexible linker (*16*, *27*, *28*), ^{1}H-^{15}N heteronuclear single quantum coherence (HSQC) spectra of the two half-

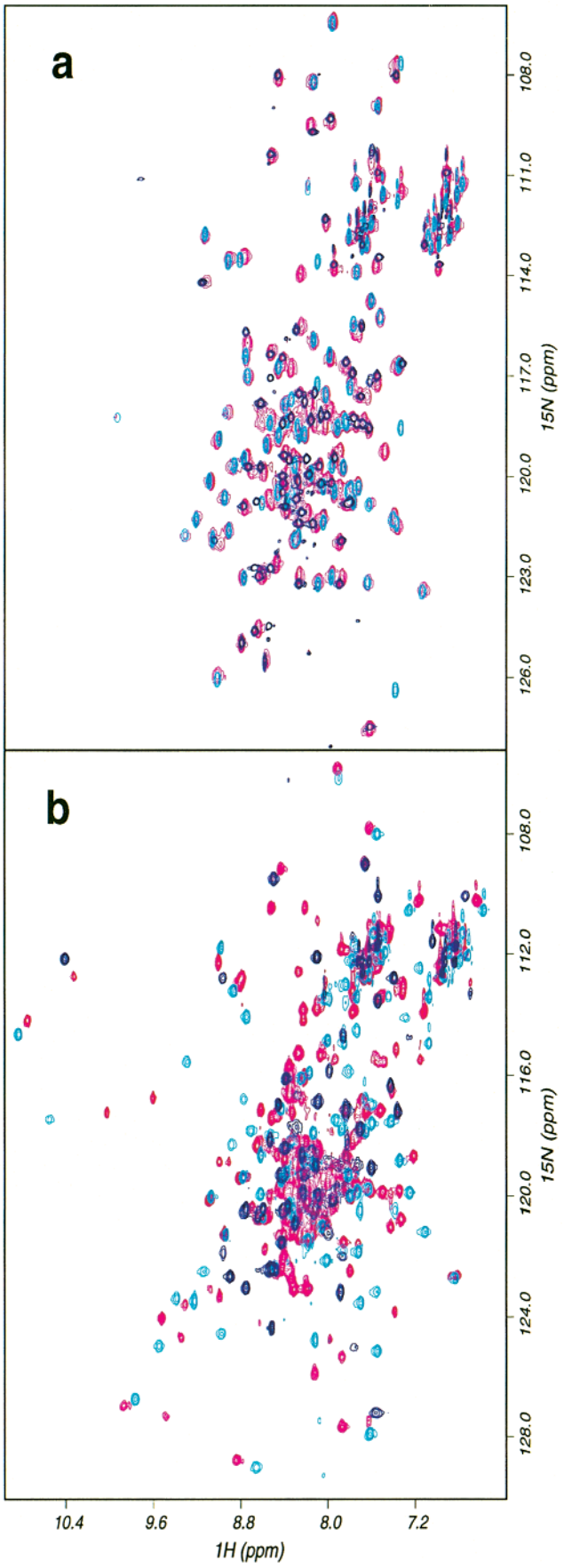

FIGURE 1: Superimposed ^{1}H-^{15}N HSQC spectra of whole yCaM (magenta) and its half-molecule fragments, yTr1(cyan) and yTr2 (blue), in the apo state (a) and the Ca^{2+}-bound state (b). All spectra were taken on NMR samples containing 0.5 mM protein. The few peaks in the spectra of the half-molecule fragments that do not superimpose on peaks in the whole apo yCaM spectrum are from those residues near the new N- and C-termini of the half-molecule fragments, consistent with the spectral effects from the expected helix-fraying.

molecule fragments of vertebrate calmodulin, vTr1 and vTr2, recapitulate the ^{1}H-^{15}N HSQC spectrum of the intact vCaM molecule: virtually all peaks of vTr1 and vTr2 superimpose on the corresponding peaks in the vCaM spectrum (data not shown). This close spectral correspondence holds for both the apo and Ca^{2+}-bound forms of vCaM. As shown in Figure 1a, the spectral correspondence between the half-molecule fragments and the intact protein holds for apo yCaM. In contrast, the ^{1}H-^{15}N HSQC spectra of Ca^{2+}-yTr1 and Ca^{2+}-yTr2 do not superimpose well on that of Ca^{2+}-yCaM (Figure 1b), indicating that the individual domains are different in the context of the whole Ca^{2+}-yCaM protein.

The spectral differences observed between the isolated half-molecule fragments and intact Ca^{2+}-yCaM could be due to (1) differences in the structures of the globular domains outside the context of the full protein or (2) the presence of interdomain interactions in Ca^{2+}-yCaM that are lost in the isolated fragments. To test for the latter possibility, ^{15}N-labeled Ca^{2+}-yTr1 was titrated with increasing amounts of unlabeled Ca^{2+}-yTr2. The reciprocal experiment was performed with ^{15}N-labeled Ca^{2+}-yTr2 and unlabeled Ca^{2+}-yTr1. In each case, significant spectral perturbations were observed (Figure 2). Cross-peaks of ^{15}N-labeled Ca^{2+}-yTr1 shift progressively with increasing amounts of Ca^{2+}-yTr2. Similar behavior is observed for side chain resonances in the spectrum as well as backbone cross-peaks. A superposition of the spectrum of Ca^{2+}-yCaM on the Ca^{2+}-yTr1 ^{1}H-^{15}N titration series reveals that the Ca^{2+}-yTr1 peaks shift toward whole Ca^{2+}-yCaM peak positions (Figure 2a), indicating that the presence of high concentrations of Ca^{2+}-yTr2 in a sample of Ca^{2+}-yTr1 mimics the state of the N-terminal domain in the intact protein.

As illustrated in Figure 2b−f, the spectral perturbations observed when unlabeled Ca^{2+}-yTr1 is added to ^{15}N-labeled Ca^{2+}-yTr2 occur in the slow exchange regime. Cross-peaks disappear from the spectrum, while new cross-peaks simultaneously appear at their final chemical shift position and continuously increase in intensity with increasing amounts of Ca^{2+}-yTr1. Similar to the Ca^{2+}-yTr1 titration, virtually all of the new Ca^{2+}-yTr2 peaks appear at Ca^{2+}-yCaM peak positions. Thus, these titrations provide direct evidence that the N-terminal and C-terminal domains of Ca^{2+}-yCaM interact, possibly inducing conformational changes within each domain.

As the affinity between Ca^{2+}-yTr1 and Ca^{2+}-yTr2 must be the same in both titration experiments, the observation of fast exchange for yTr1 and slow exchange for yTr2 must arise from larger chemical shift perturbations experienced by the Ca^{2+}-yTr2 peaks relative to those experienced by Ca^{2+}-yTr1 peaks (*29*). The behavior of individual peaks bear this out: for example, Gly 131 differs in its spectral position in the spectra of Ca^{2+}-yTr1 and of Ca^{2+}-yCaM by 191 Hz vs a difference of only 42 Hz for Gly 59, the analogous residue in the N-terminal domain.

The high protein concentrations ($\sim 10^{-3}$ M) used in NMR experiments along with the known hydrophobic nature of the Ca^{2+}-bound form of CaM raised concerns about the specificity of the interactions revealed in the NMR titrations.

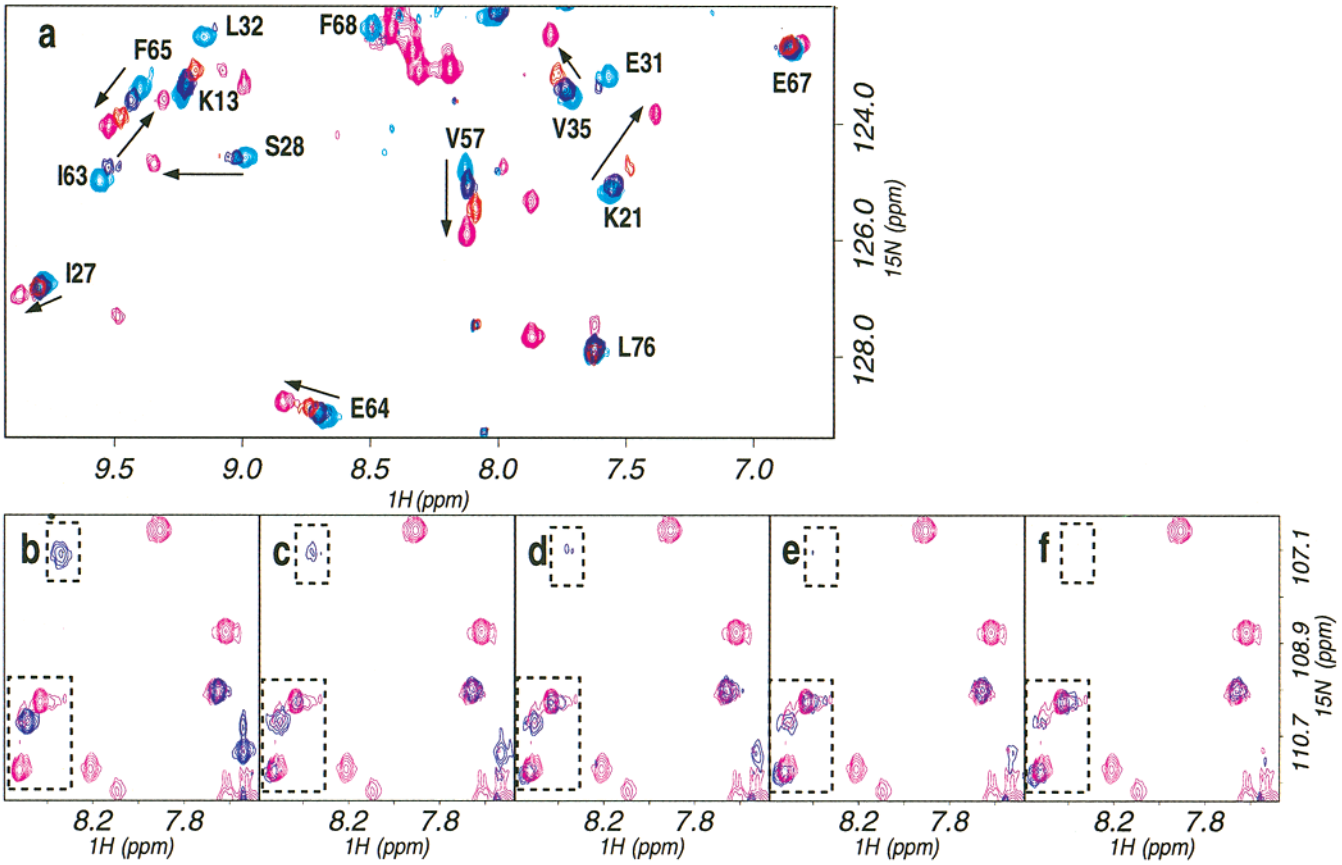

FIGURE 2: Superimposed regions of the ^{1}H-^{15}N HSQC spectra from the ^{15}N-labeled Ca^{2+}-yTr1(a) and ^{15}N-labeled Ca^{2+}-yTr2 (b−f) titration experiments. In all panels, the corresponding region from the spectrum of whole Ca^{2+}-yCaM (magenta) is also superimposed. Panel a consists of identical regions from the ^{1}H-^{15}N HSQC spectra of ^{15}N-labeled Ca^{2+}-yTr1 titrated with 0 (cyan), 4 (blue), and 17 (red) equivalents of unlabeled Ca^{2+}-yTr2. Arrows in panel a highlight the direction of the chemical shift perturbations as well as point to the corresponding Ca^{2+}-yCaM peak. Each panel of b−f consists of identical regions from the ^{1}H-^{15}N HSQC spectra of ^{15}N-labeled Ca^{2+}-yTr2 (blue) titrated with 0 (b), 4 (c), 7.5 (d), 10 (e), and 14 (f) equivalents of unlabeled Ca^{2+}-yTr1. Dashed boxes highlight peaks that either disappear or appear during the titration.

Our lab has previously demonstrated the use of heterologous proteins to establish the specificity and functional significance of protein−protein interactions observed by NMR (*30*, *31*). Addition of the vertebrate analogue, Ca^{2+}-vTr2, to ^{15}N-labeled Ca^{2+}-yTr1 did not perturb the ^{1}H-^{15}N HSQC spectrum, even at high concentrations (data not shown). This result establishes that the interaction between Ca^{2+}-yTr1 and Ca^{2+}-yTr2 is remarkably specific.

To distinguish between an intramolecular or intermolecular interaction between N- and C-terminal domains, ^{1}H-^{15}N HSQC spectra were collected of Ca^{2+}-yCaM at 1.2 mM and 0.25 mM. All peaks in the two spectra superimpose and their line widths are indistinguishable, indicating that the interaction is not intermolecular (data not shown).[2]

To estimate the binding affinity between Ca^{2+}-yTr1 and Ca^{2+}-yTr2, chemical shift perturbations of Ca^{2+}-yTr1 peaks were plotted as a function of [Ca^{2+}-yTr2]. Each binding curve was fit to a simple bimolecular binding model, yielding K_d values of 5−15 mM (*26*). Figure 4 shows binding curves of residues located in the four α-helices of Ca^{2+}-yTr1. Intriguingly, calmodulin's flexible central linker is predicted to produce a local effective concentration of the two globular domains of 15 mM, making this high "ligand" concentration an intrinsic property of the calmodulin molecule that is independent of the total protein concentration (*32*). Consequently, the close match between the measured K_d and the effective local concentration yields an intramolecular binding equilibrium in which a significant proportion of Ca^{2+}-yCaM molecules will exist with their domains interacting in vivo as well as in vitro, making this intramolecular interaction physiologically relevant.

Chemical shift perturbation mapping is widely used to identify binding sites in protein−protein interactions (*31*, *33*−*35*). We, therefore, assigned the ^{1}H-^{15}N HSQC spectrum of Ca^{2+}-yTr1 (see Methods) to define its binding surface with the C-terminal domain. Although a majority of Ca^{2+}-yTr1 peaks display measurable chemical shift perturbations, a subset of peaks exhibit significant intensity loss early in the titration. The resonance broadening indicates that these peaks experience the largest chemical shift changes among all Ca^{2+}-yTr1 peaks, and thus, the corresponding residues are likely to comprise the binding interface (*33*, *35*). By these criteria, residues that comprise the binding interface of Ca^{2+}-yTr1 include Phe 12, Ala 15, Phe 16, Ala 17, Leu 18, Phe 19, Leu 32, Ile 55, Phe 68, Ile 63, and Met 72, indicating that the interaction between domains is hydrophobic in nature. When mapped onto the structure of a model based on the N-terminal domain of Ca^{2+}-vCaM, the majority of these residues define a contiguous surface (Figure 3). Interestingly,

[2] The average ^{15}N line width for the spectra were 13.3 Hz vs 14.1 Hz, at the lower and higher protein concentrations, respectively, and no single peak's line width varied between the two spectra by more than 2 Hz.

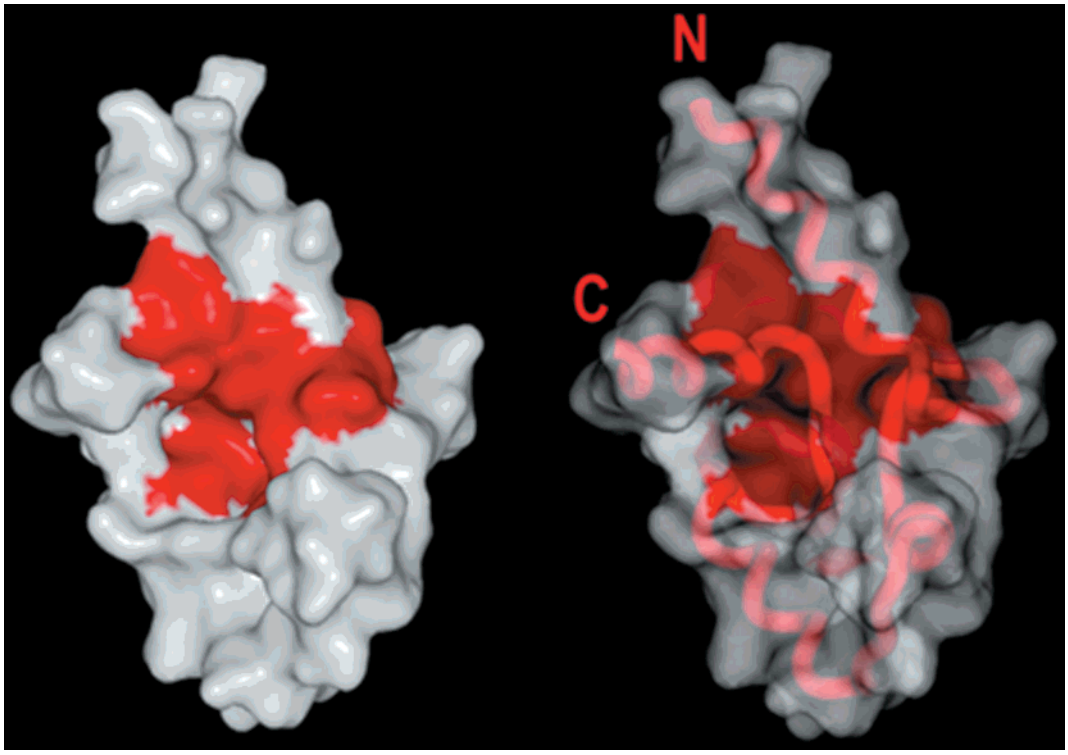

FIGURE 3: Model of the proposed Ca^{2+}-yTr2 binding site of Ca^{2+}-yTr1. A structural model of Ca^{2+}-yTr1 was constructed based on the X-ray structure of Ca^{2+}-vCaM (1CLL). Side chains of residues that differ between vCaM and yCaM were substituted with the yCaM residue. Residues corresponding to peaks whose intensities decreased by greater than 50% after the addition of 1 equivalent of unlabeled Ca^{2+}-yTr2 are highlighted in red on the protein molecular surface and are noted in the text. The worm backbone (right) and molecular surface (left) are in identical orientation. These figures were created using SPOCK. (J. A. Christopher, Department of Biochemistry, Texas A&M University, College Station, TX).

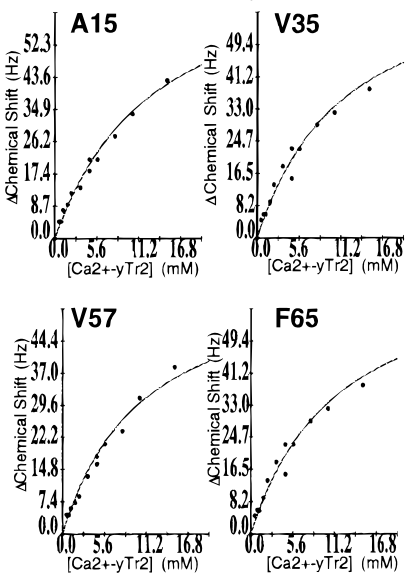

FIGURE 4: Titration curves for Ala 15, Val35, Val57, and Phe 65 from the ^{15}N-labeled Ca^{2+}-yTr1 titration experiment. Titration curves display the change in the chemical shift of the ^{1}H-^{15}N HSQC peak corresponding to the given residue as a function of increasing unlabeled Ca^{2+}-yTr2. The line drawn through the experimental points is the fitted binding curve obtained from xcrvfit.

this binding surface partially overlaps with the hydrophobic pocket used by Ca^{2+}-vCaM to bind to target peptides and small drug molecules (*36*, *37*). In addition, the fact that residues of the binding interface arise from all four α-helices within the N-terminal domain may explain why spectral perturbations are observed throughout the entire domain.

Asp 20 and Glu 31, the first and last liganding residues of Ca^{2+}-binding loop I, also broaden out early in the Ca^{2+}-yTr1 titration. These residues follow and precede Phe 19 and Leu 32, both of which are in the binding site for Ca^{2+}-yTr2. Our data suggest that Ca^{2+} binding and the interdomain interaction are linked in yCaM, consistent with the observation that Ca^{2+} binding is weaker in the isolated half-molecule yCaM fragments than it is in the intact protein (*21*). A similar observation was made in parvalbumin where two fragments comprising the AB domain and the two EF-hand site CD·EF domain form a noncovalent complex possessing higher Ca^{2+} affinity than the individual fragments (*38*).

Our data provide direct evidence of an interaction between the two globular domains of Ca^{2+}-yCaM, suggesting that the protein exists in a collapsed or compact state. This is in contrast to the extended state of Ca^{2+}-vCaM with its two independent domains (*19*). Other examples of proteins possessing four EF-hands that exist in a collapsed rather than extended state include sarcoplasmic Ca^{2+}-binding protein and recoverin (*39*, *40*). We note that, like yCaM, these proteins each have at least one nonfunctional Ca^{2+}-binding site. It has been shown that (1) the presence of an EF-hand site that is unable to bind Ca^{2+} hinders the ability of a two-site domain to undergo the conformational change to the open state, and (2) binding of a target peptide can induce a conformational change to the open state (*41*, *42*). Therefore, the functional significance of the interdomain interaction in Ca^{2+}-yCaM may involve stabilization of the open conformation of a domain that includes a nonfunctional Ca^{2+} site. This hypothesis is consistent with the decreased Ca^{2+} binding affinity exhibited by EF-hand site III (site IV is nonfunctional) in yTr2 compared to whole yCaM (*21*). Because the conformational change from the closed to open state is linked to

Ca^{2+} binding, the lower Ca^{2+} affinity of the C-terminal half of yCaM is likely to be accompanied by a compromised ability to convert to the open state (*5*). A destabilized open state in the C-terminal domain is consistent with the larger chemical shift perturbations experienced by Ca^{2+}-yTr2 relative to Ca^{2+}-yTr1 during the respective titrations. We propose that Ca^{2+}-yTr2 undergoes a larger structural change as a result of the interdomain interaction because Ca^{2+}-yTr1 is close to if not already in the open Ca^{2+}-bound conformation, while Ca^{2+}-yTr2, with its single functional Ca^{2+}-binding site, is not.

The results presented here clearly show that the structure of Ca^{2+}-yCaM must be significantly different from that of Ca^{2+}-vCaM, since the two domains of Ca^{2+}-yCaM interact to yield a collapsed state. Our working model consisting of a compact conformation for Ca^{2+}-yCaM in which the open state of the C-terminal domain is stabilized via favorable interactions available on the hydrophobic surface of the open conformation of the N-terminal domain provides some structural insight on previously published circular dichroism and X-ray scattering data that have suggested that the Ca^{2+}-bound structure of yCaM differs from that of vCaM (*18*, *21*). The prevalence of this compact state of Ca^{2+}-yCaM raises intriguing questions about the mechanism of action of yCaM with its Ca^{2+}-dependent target proteins, since the interdomain interaction site appears to overlap with the putative target proteins binding site, as identified in Ca^{2+}-vCaM. This observation may explain why Ca^{2+}-yCaM is significantly less effective at binding and activating vCaM's target protein, since the competition between the binding of a vCaM target and the interdomain binding in Ca^{2+}-yCaM could lower the apparent affinity. The physiological consequences of this novel Ca^{2+}-yCaM conformation will be revealed as the structures and mechanisms of bona fide Ca^{2+}-dependent target proteins from yeast are revealed.

ACKNOWLEDGMENT

We thank P. Rajagopal for her assistance with NMR experiments; M. Shea for the generous gift of the vTr1 and vTr2 expression systems; T. N. Davis and Q. Yi for critical reading of the manuscript, and M. Brown for purification of the ^{15}N-labeled vCaM samples and the construction of the structural model of Ca^{2+}-yTr1 via SPOCK.

REFERENCES

1. Cohen, P., and Klee, C. B. (1988) *Calmodulin*, Molecular Aspects of Cellular Regulation, Vol. 5, Elsevier, Amsterdam.
2. Carafoli, E., and Claude, K. (1992) *New Developments in the Calmodulin Field*, Cell Calcium, Vol. 13, University of Sheffield Biomedical Information Service, Sheffield.
3. Rogers, M. S., and Strehler, E. E. (1996) in *Guidebook to the Calcium-Binding Proteins* (Celio, M. R., Pauls, T., and Schwaller, B., Eds.), pp 34−42 Oxford University Press, Oxford.
4. Eldik, L. V., and Watterson, D. M. (1998) *Calmodulin and Signal Transduction*, Acadmic Press, San Diego.
5. LaPorte, D. C., Wierman, B. M., and Storm, D. R. (1980) *Biochemistry 19*, 3814−9.
6. Moncrief, N. D., Kretsinger, R. H., and Goodman, M. (1990) *J. Mol. Evol. 30*, 522−62.
7. Davis, T. N., Urdea, M. S., Masiarz, F. R., and Thorner, J. (1986) *Cell 47*, 423−31.
8. Luan, Y., Matsuura, I., Yazawa, M., Nakamura, T., and Yagi, K. (1987) *J. Biochem. (Tokyo) 102*, 1531−7.
9. Starovasnik, M. A., Davis, T. N., and Klevit, R. E. (1993) *Biochemistry 32*, 3261- 70.
10. Matsuura, I., Ishihara, K., Nakai, Y., Yazawa, M., Toda, H., and Yagi, K. (1991) *J. Biochem. (Tokyo) 109*, 190−7.
11. Brockerhoff, S. E., Edmonds, C. G., and Davis, T. N. (1992) *Protein Sci. 1*, 504−16.
12. Linse, S., Helmersson, A., and Forsen, S. (1991) *J. Biol. Chem. 266*, 8050−4.
13. Ohya, Y., Uno, I., Ishikawa, T., and Anraku, Y. (1987) *Eur. J. Biochem. 168*, 13−9.
14. Davis, T. N., and Thorner, J. (1989) *Proc. Natl. Acad. Sci. U.S.A. 86*, 7909−13.
15. Matsuura, I., Kimura, E., Tai, K., and Yazawa, M. (1993) *J. Biol. Chem. 268*, 13267−73.
16. Zhang, M., Tanaka, T., and Ikura, M. (1995) *Nat. Struct. Biol. 2*, 758−67.
17. Kuboniwa, H., Tjandra, N., Grzesiek, S., Ren, H., Klee, C. B., and Bax, A. (1995) *Nat. Struct. Biol. 2*, 768−76.
18. Yoshino, H., Izumi, Y., Sakai, K., Takezawa, H., Matsuura, I., Maekawa, H., and Yazawa, M. (1996) *Biochemistry 35*, 2388−93.
19. Barbato, G., Ikura, M., Kay, L. E., Pastor, R. W., and Bax, A. (1992) *Biochemistry 31*, 5269−78.
20. Trewhella, J. (1992) *Cell Calcium 13*, 377−390.
21. Nakashima, K., Ishida, H., Ohki, S. Y., Hikichi, K., and Yazawa, M. (1999) *Biochemistry 38*, 98−104.
22. Klevit, R. E., Dalgarno, D. C., Levine, B. A., and Williams, R. J. (1984) *Eur. J. Biochem. 139*, 109−14.
23. Sorensen, B. R., and Shea, M. A. (1998) *Biochemistry 37*, 4244−53.
24. Serpersu, E. H., Shortle, D., and Mildvan, A. S. (1986) *Biochemistry 25*, 68−77.
25. Ohki, S., Miura, K., Saito, M., Nakashima, K., Maekawa, H., Yazawa, M., Tsuda, S., and Hikichi, K. (1996) *J. Biochem. 119*, 1045−55.
26. McKay, R. T., Tripet, B. P., Hodges, R. S., and Sykes, B. D. (1997) *J. Biol. Chem. 272*, 28494−500.
27. Chattopadhyaya, R., Meador, W. E., Means, A. R., and Quiocho, F. A. (1992) *J. Mol. Biol. 228*, 1177−92.
28. Finn, B. E., Evenas, J., Drakenberg, T., Waltho, J. P., Thulin, E., and Forsen, S. (1995) *Nat. Struct. Biol. 2*, 777−83.
29. Roberts, G. C. K. (1993) *NMR of Macromolecules: A Practical Approach*, 1st ed., The Practical Approach Series, (Rickwood, D., and Hames, B. D., Eds.) IRL Press at Oxford University Press, Oxford.
30. Rajagopal, P., Waygood, E. B., Reizer, J., Saier, M. H., Jr., and Klevit, R. E. (1997) *Protein Sci. 6*, 2624−7.
31. Jones, B. E., Dossonnet, V., Kuster, E., Hillen, W., Deutscher, J., and Klevit, R. E. (1997) *J. Biol. Chem. 272*, 26530−5.
32. Finn, B. E., and Forsen, S. (1995) *Structure 3*, 7−11.
33. Rajagopal, P., and Klevit, R. E. (1994) in *Techniques in Protein Chemistry* Vol. 5, pp. 439−445, Academic Press, San Diego.
34. Jensen, P. H., Soroka, V., Thomsen, N. K., Ralets, I., Berezin, V., Bock, E., and Poulsen, F. M. (1999) *Nat. Struct. Biol. 6*, 486-93.
35. Dekker, N., Cox, M., Boelens, R., Verrijzer, C. P., van der Vliet, P. C., and Kaptein, R. (1993) *Nature 362*, 852−5.
36. Crivici, A., and Ikura, M. (1995) *Annu. Rev. Biophys. Biomol. Struct. 24*, 85−116.
37. Vandonselaar, M., Hickie, R. A., Quail, J. W., and Delbaere, L. T. (1994) *Nat. Struct. Biol. 1*, 795−801.
38. Permyakov, E. A., Medvedkin, V. N., Mitin, Y. V., and Kretsinger, R. H. (1991) *Biochim. Biophys. Acta 1076*, 67−70.
39. Cook, W. J., Jeffrey, L. C., Cox, J. A., and Vijay-Kumar, S. (1993) *J. Mol. Biol. 229*, 461−71.
40. Ames, J. B., Ishima, R., Tanaka, T., Gordon, J. I., Stryer, L., and Ikura, M. (1997) *Nature 389*, 198−202.
41. Evenas, J., Forsen, S., Malmendal, A., and Akke, M. (1999) *J. Mol. Biol. 289*, 603−17.
42. Li, M. X., Spyracopoulos, L., and Sykes, B. D. (1999) *Biochemistry 38*, 8289−98.

BI992697A